FIRST INSERTION DEVICE FOR SPRING-8 LONG STRAIGHT SECTIONS

T. Hara*, T. Tanaka, K. Tamasaku, T. Ishikawa and H. Kitamura,
SPring-8/RIKEN, Mikazuki, Hyogo 679-5148, Japan
M. Yabashi, T. Bizen, T. Seike, X-M. Maréchal and S. Goto,
SPring-8/JASRI, Mikazuki, Hyogo 679-5198, Japan

Abstract

In the summer of 2000, a 25 m-long insertion device was installed in one of the four 30 m-long straight sections in the SPring-8 storage ring. The 25 m undulator has 780 magnetic periods ranged continuously inside a vacuum chamber. The commissioning of the undulator and beamline was started in November 2000. The undulator radiation flux and spectrum were measured and they agree with theoretical results. Except a lifetime reduction at small gaps, expected performance of the undulator was achieved.

1 INTRODUCTION

"High brilliance" is the characteristic which all third-generation synchrotron radiation sources are pursuing for. Since radiation from undulators is enhanced at specific photon energies due to an interference effect, we can obtain high brilliance radiation at these energies. Thus, the undulators become radiation sources mainly used at third-generation facilities. If one wants to increase further the brilliance using the same electron beam, it can be achieved by increasing the number of undulator periods. In most storage rings, the length of undulators is limited by a physical boundary, i.e. the length of straight sections.

SPring-8 is a unique third-generation light source possessing four 30 m-long straight sections to realize super-brilliant synchrotron radiation sources. In the summer of 2000, the storage ring lattice was changed and all focusing magnets were removed from the long straight sections [1]. At the same time, we have installed the first long insertion device for the beamline BL19LXU. The type of the long insertion device is an in-vacuum X-ray undulator with 780 magnetic periods of 32 mm. The undulator magnets are ranged continuously for 25 m without any gap between magnet blocks. The magnet structure is the same as the SPring-8 standard type in-vacuum undulators, which have been successfully operated for more than five years at SPring-8 [2].

2 25M-LONG IN-VACUUM UNDULATOR

2.1 In-Vacuum Undulators

The reduction of the undulator periodic length contributes to the increase of the number of periods and brilliance. However, it results in the use of small magnet blocks, and undulator operation at small magnetic gaps becomes inevitable in order to obtain sufficient magnetic fields. In-vacuum undulators housing magnet arrays inside a vacuum chamber have an advantage over conventional out of vacuum undulators to achieve small gaps, because there is no gap loss due to chamber walls and a full magnetic gap can be used as a physical aperture for electron beams. On the other hand, the magnets of the in-vacuum undulator should be ultra-high vacuum compatible and special care is necessary in its design to minimize disturbance of the electron beam.

Figure 1 shows a schematic of the in-vacuum undulator developed at SPring-8. The diameter of the vacuum chamber is about 30 cm. The magnet arrays are supported by H-shaped iron beams through bellows, and the bellows allow the magnetic gap movement.

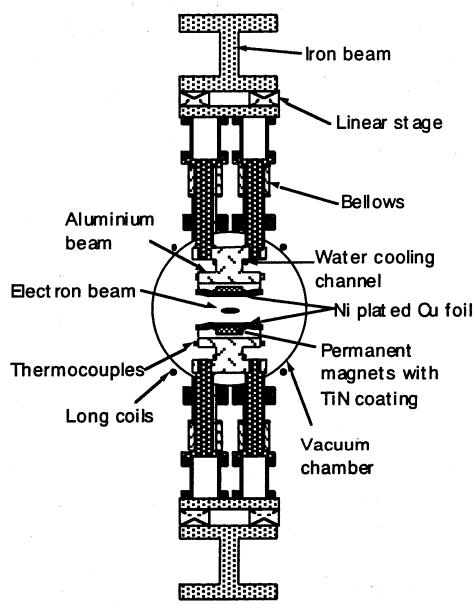

Figure 1: Schematic view of the SPring-8 in-vacuum undulator cross section.

*toru@spring8.or.jp

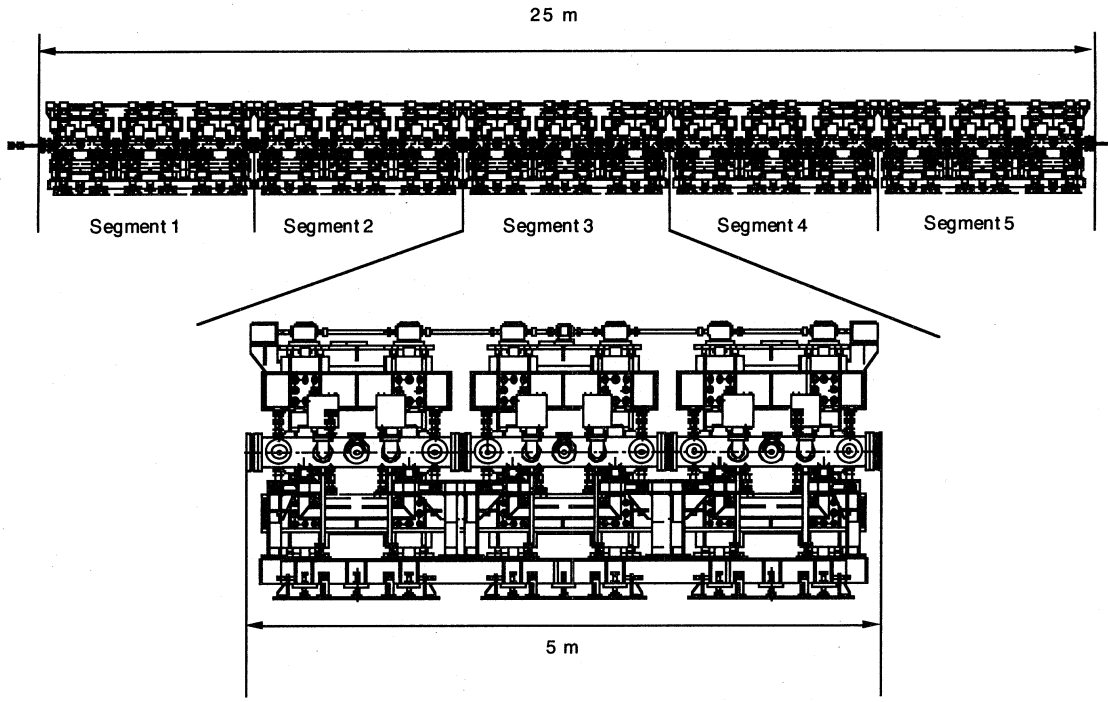

Figure 2: 25 m in-vacuum undulator structure consisting of five segments.

Magnetic field measurements and corrections are carried out without the vacuum chamber [3]. After finishing them, the magnets and Al-beams are once removed, and the chamber is installed. Then the magnet arrays are slid into the chamber from the side and fixed to the iron beams.

In order to reduce the effect on the electron beam, the rugged surface of the magnet blocks is covered with a Ni (15 μm) plated Cu (50 μm) foil. Cu is used to reduce electric resistance for image currents of the beam, and Ni assures a physical contact to the magnets utilizing magnetism. When the electron beam passes through the undulator, the Cu+Ni foil is heated due to the resistive wall effect [4, 5]. In order to remove the heat produced at the foil, the undulator magnets have a water cooling pipes (Fig. 1) to control the magnet temperature at 25 ± 0.2 °C. The stabilization of the magnet temperature also helps to prevent a thermal variation of the magnetic field (~ 0.1 %/°C).

At both extremities of the undulator, water cooled RF flexible tapers connect the magnet arrays and neighboring ring chambers [5]. They are flexible against the undulator gap movement and smoothly transform the cross sections to reduce beam impedance.

2.2 Mechanical structure of the 25 m in-vacuum undulator

The 25 m-long undulator consists of five segments (Fig. 2) and each segment has similar structure to the 4.5 m-long in-vacuum undulators already installed and successfully operated for years at SPring-8. The undulator gap is driven by five stepping motors attached to each segment, but tapering between segments is not considered and the five gaps are changed simultaneously.

The field measurements and corrections were carried out by the segment. Later, two segments were assembled and the measurements and corrections were repeated at the connecting points between the segments [6].

The top and bottom magnet arrays are continuously ranged for 25 m and there is no gap between segments. This is another advantage of the in-vacuum type over out of vacuum undulators, when constructing a long undulator. The vacuum chambers are connected externally using bellows, therefore there is no interference with the magnet arrays as shown in Fig. 3 (a). In case of the out of vacuum undulators, it is inevitable that the magnet arrays are separated by vacuum flanges (Fig. 3 (b)) unless using a 25 m-long vacuum chamber. Continuous magnet arrays not only enables the use of a full length of the straight section, but also it eliminates a radiation phase matching scheme.

2.3 Vacuum System

The vacuum system of the 25 m in-vacuum undulator consists of sixty NEG (Non Evaporable Getter) pumps and thirty ion pumps having total pumping speed of 34000 l/sec. To attain an ultra-high vacuum of 10^{-9} Pa

order, it is inevitable to bake out the undulator. In addition to a high pumping speed, all components installed in the vacuum are carefully designed and fabricated. The magnet blocks are coat with TiN to prevent outgas and oxidation of the surface, and they are pre-baked at 145 °C before assembled to the magnet array. During the undulator bake out of 48 hours, the temperature of the chamber is kept at 200 °C, while the magnet temperature is controlled at 125 °C to avoid irreversible demagnetization. Once the magnets are thermally stabilized at 145 °C during the pre-bake out, further field change during the bake-out at 125 °C is negligible. In case of the 25 m undulator, thermal expansion reaches 3.5 cm at both ends of the undulator. In order to avoid a break in vacuum components, they sit on linear stages with freedom for longitudinal movements.

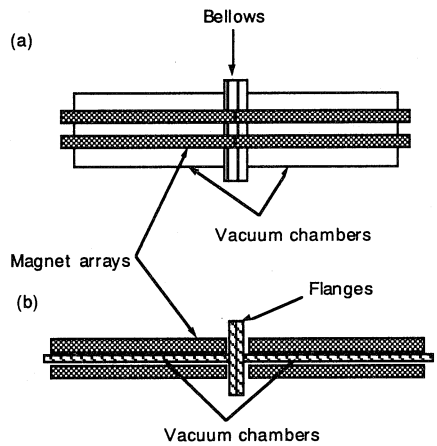

Figure 3: Schematics of the magnet array connections for a long undulator, (a) in-vacuum type, (b) out of vacuum type.

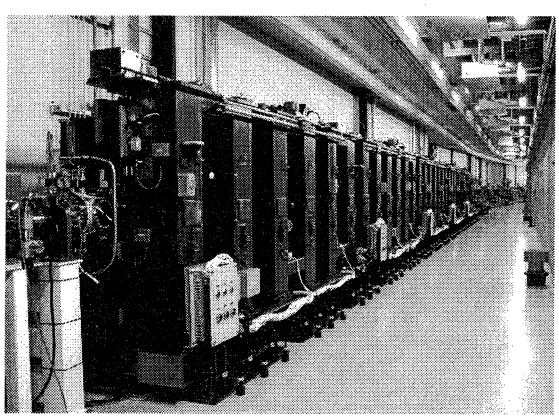

Figure 4: The 25 m in-vacuum undulator installed in the SPring-8 storage ring.

2.4 Installation in the storage ring

Figure 4 is a photograph of the 25 m in-vacuum undulator installed in the SPring-8 storage ring. The undulator was transported by the segment and assembled inside the ring tunnel. After the bake out, the vacuum of < 2×10^{-8} Pa was achieved.

Parameters of the undulator and the electron beam are listed in table 1.

2.5 Expected brilliance of the 25 m undulator

Theoretical brilliance of the 25 m undulator is about five times higher than that of the 4.5 m-long standard in-vacuum undulators at SPring-8 (Fig. 5). One may expect a quadratic increase of the brilliance with the undulator length L, but it is not the case at SPring-8. Since flux density *FD* and brilliance *B* is described as

$$FD = \frac{F}{\Sigma_{x'}\Sigma_{y'}}, \quad B = \frac{F}{\Sigma_{x'}\Sigma_{y'}\Sigma_x\Sigma_y},$$

where Σ_x, $\Sigma_{x'}$, Σ_y and $\Sigma_{y'}$ are horizontal (x) and vertical (y) RMS source sizes and divergences, which are convolution of the electron beam and the photon diffraction limit. *F* is the number of emitted photons in a narrow relative band (often 0.1%) per second, and it increases with L if the undulator periodic length is the same. If the electron beam is much larger than the photon diffraction limit, *FD* and *B* increase proportionally to L, since Σ_x, $\Sigma_{x'}$, Σ_y and $\Sigma_{y'}$ do not change as L. In case of zero electron beam emittance, source sizes and divergences are determined by the photon diffraction limit, which are

$$\Sigma_x = \Sigma_y \approx \frac{\sqrt{2\lambda L}}{4\pi}, \quad \Sigma_{x'} = \Sigma_{y'} \approx \sqrt{\frac{\lambda}{2L}},$$

where λ is the photon wavelength [7]. In this case, *FD* increases as L^2, but *B* is just proportional to L because Σ_x, $\Sigma_y \propto \sqrt{L}$.

In case of the SPring-8 4.5 m and 25 m undulators, the photon diffraction limit (for example 6 μm and 1.6 μrad at 10 keV) dominates only $\Sigma_{y'}$ as shown in table 1, so *FD*, $B \propto L^{1.5}$. However, a large vertical beta function at the 25 m undulator (β_y = 14.44 m), compared with that at the 4.5 m undulators (β_y = 5.77m), reduces the increase of the brilliance to $B \propto L$.

3 COMMISIONING OF THE 25M IN-VACUUM UNDULATOR

From the end of November 2000, we started the commissioning of BL19LXU including the 25 m in-vacuum undulator.

Table 1: Parameters of the 25m long in-vacuum undulator and the electron beam at the long straight section.

Undulator	
Type	Pure permanent magnet (halbach)
Periodic length (mm)	32
Number of periods	780
Gap range (mm)	12~50
Maximum K	1.76 at 12 mm gap
Photon energy of fundamental radiation (keV)	7.4~18
Total power with 12 mm gap (kW)	35
Electron beam	
Energy (GeV)	8
RMS horizontal size (μm) and angular divergence (μrad)	370 and 16
RMS vertical size (μm) and angular divergence (μrad)	9 and 0.6
Maximum current (mA)	100

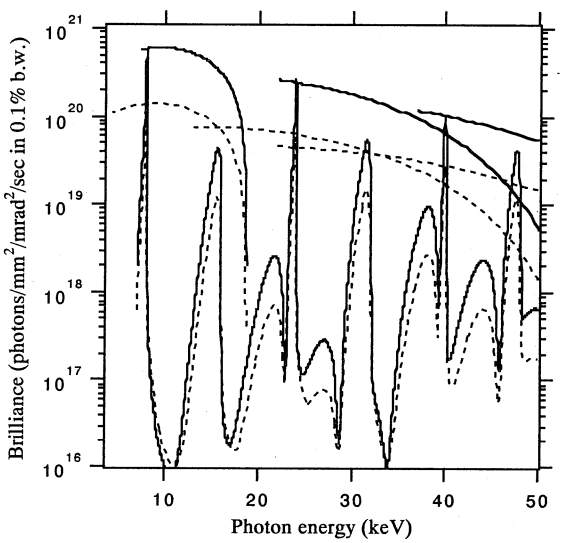

Figure 5: Theoretical brilliance of the BL19LXU 25 m in-vacuum undulator (solid lines) and the BL29XU 4.5 m in-vacuum undulator (dotted lines) at SPring-8. Spectra shown is calculated for the first harmonic photon energy of 7.5 keV.

3.1 Effect on the electron beam

A choice of the vertical betatron function β_y determines the beam lifetime performance at small undulator gaps. The optimum vertical betatron function at the undulator center is β_{y0}=L/2 (L is an undulator length) [8], and the vertical betatron function at the 25 m undulator (β_{y0} = 14.44 m) was set close to the optimum value. Even though, because of large β_y compared to the normal 5 m-long straight sections (β_{y0} = 5.77 m), 30 % lifetime reduction was observed when the undulator is closed to the minimum gap of 12 mm (Fig. 6).

Figure 7 shows the vertical tune shift with respect to the undulator gap. Observed tune shift agrees with the theoretical natural vertical focusing of the undulator provided by the wiggle electron motion and the longitudinal field in the undulator. It is inherent to any conventional planar undulator. Tune shift due to the multi-pole field components of the undulator was negligible.

The electron beam orbit distortion associated with the undulator gap change was corrected within a few μm using two pairs of steering coils attached at the both extremities of the undulator.

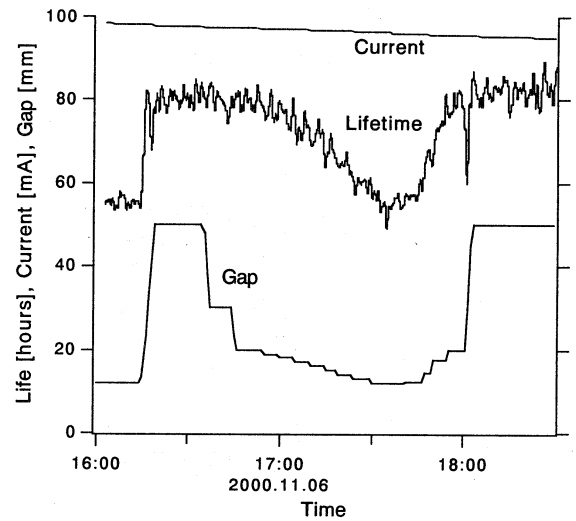

Figure 6: Beam lifetime as a function of the 25 m undulator gap. 80 hours at 50 mm gap is the lifetime with other 4.5 m undulator gaps closed under multi-bunch ring operation.

3.2 Beam orbit in the undulator

In order to roughly estimate the difference between the longitudinal undulator axis and the beam orbit, we produced an parallel orbit bump in the vertical direction, and measured the undulator radiation energy and beam lifetime. We assumed that the beam passes parallel to the longitudinal undulator axis. The results are shown in Fig. 8. From the polynomial fits, we confirmed that the beam passes slightly (0.1 ~ 0.2 mm) above the undulator axis.

Because of its long length, small environmental fields, such as a geomagnetic field, may affect the undulator spectrum. The observed spectrum with a small K-value (50 mm gap) was broad and shifted toward lower energies compared to the theoretical spectrum. When a uniform horizontal field of 0.1 G was applied over the 25 m length, the spectral shape reverted to the theoretical shape. It indicates that the electron beam orbit deviates vertically by ~30 μm. As a matter of fact, the direction of the undulator, in which the field corrections were carried out,

differed by 90 degrees from the direction of installation in the storage ring.

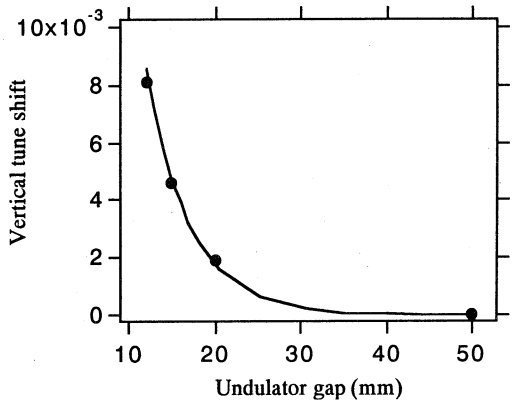

Figure 7: Measured (solid circles) and theoretical (solid line) vertical tune shift as a function of the undulator gap.

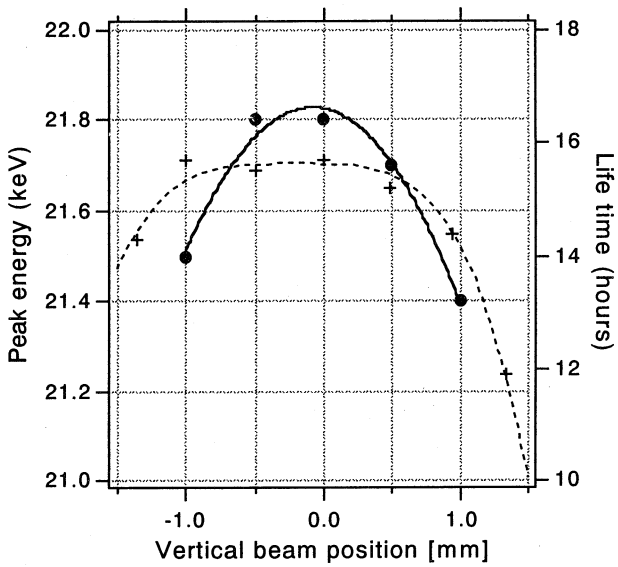

Figure 8: Peak photon energy of the third harmonics (solid circles) and the beam lifetime (crosses) as a function of the vertical beam position in the undulator. The undulator gap was set at 12 mm and the lifetime was measured with 1 mA single bunch. Lines are polynomial fits.

3.3 Radiation performance

Figure 9 is a preliminary report of the radiation spectrum demonstrating that 65~75 % of the expected flux was obtained. Under the high peak current operation mode of the SPring-8 storage ring, the undulator radiation Bose degeneracy of 1~3 can be obtained at photon energies around 8 keV.

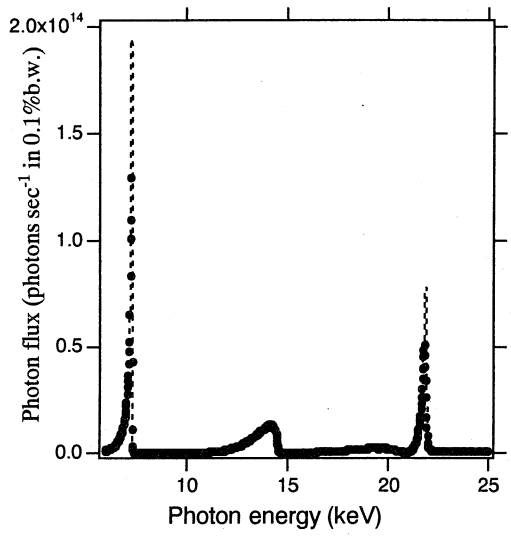

Figure 9: The undulator spectrum measured at 12 mm gap with a square slit of 3.9 μrad aperture. The solid circles are the observed flux with a calibrated PIN diode and the broken line is the calculated flux including undulator field errors.

4 CONCLUSIONS

The first 25 m in-vacuum undulator for the SPring-8 long straight sections was installed and successfully operated. The 25 m undulator not only improves the performance of the x-ray experiments currently being carried out at third generation sources, but also it provides a chance to develop new experimental schemes in the X-ray region, such as X-ray intensity correlation [9] and nonlinear phenomena.

5 REFERENCES

[1] H. Tanaka et al., Nucl. Instrum. Meth., in press.
[2] T. Hara, T. Tanaka, T. Tanabe, X.-M. Maréchal, S. Okada and H. Kitamura., J. Synchrotron Rad. **5**, 403 (1998).
[3] T. Tanaka, T. Seike and H. Kitamura, Nucl. Instrum. Meth A**465**, 600 (2001).
[4] K. Bane and S. Krinsky, Proc. 1993 IEEE Part. Accel. Conf., (1993) 3375.
[5] T. Hara, T. Tanaka, T. Tanabe, X.M. Maréchal, H. Kitamura, P. Elleaume, B. Morisson, J. Chavanne, P. Vaerenbergh and D. Schmidt, J. Synchrotron Rad. **5** (1998) 406.
[6] T. Tanaka, T. Seike, X.M. Maréchal, T. Bizen, T. Hara and H. Kitamura., Nucl. Instrum. Meth. A**467** (2001) 149.
[7] D. Attwood, K. Halbach and K. J. Kim, Science **228** (1985) 1265.
[8] H. Kitamura, J. Synchrotron Rad. **7** (2000) 121.
[9] M. Yabashi, K. Tamasaku and T. Ishikawa, Phys. Rev. Lett., in press.